

# Phase Retrieval on Undersampled Data from the Thermal Infrared Sensor (TIRS)

---

**Matthew R. Bolcar and Eric Mentzell**

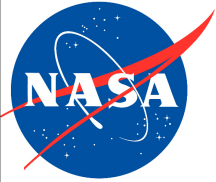
*NASA Goddard Space Flight Center, Greenbelt, MD 20771*

**Presented at:**

The Frontiers in Optics Meeting  
of  
The Optical Society of America  
*San Jose, California*

October 20, 2011

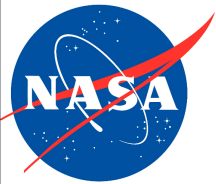
FThD4



# Outline

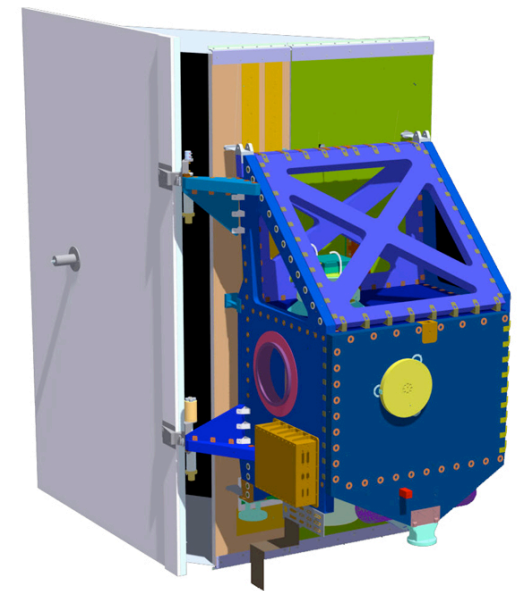
---

- TIRS Overview
- Purpose of Test
- Methods of Test
- Data
- Results
- Conclusion



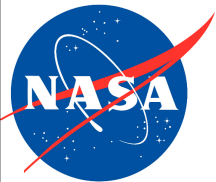
# The Thermal Infrared Sensor (TIRS)<sup>1</sup>

- Purpose:
  - One of two instruments on the Landsat Data Continuity Mission (LDCM)
  - Provide 100-m ground-resolution thermal imagery
  - Ensure continuity with previous Landsat thermal instruments
- Design:
  - Push-broom type imager
  - Refractive, 4-element telescope
  - Operates in two thermal bands: 10.9 and 12.0  $\mu\text{m}$
  - Three Quantum Well Infrared Photodetector (QWIP)<sup>2</sup> arrays



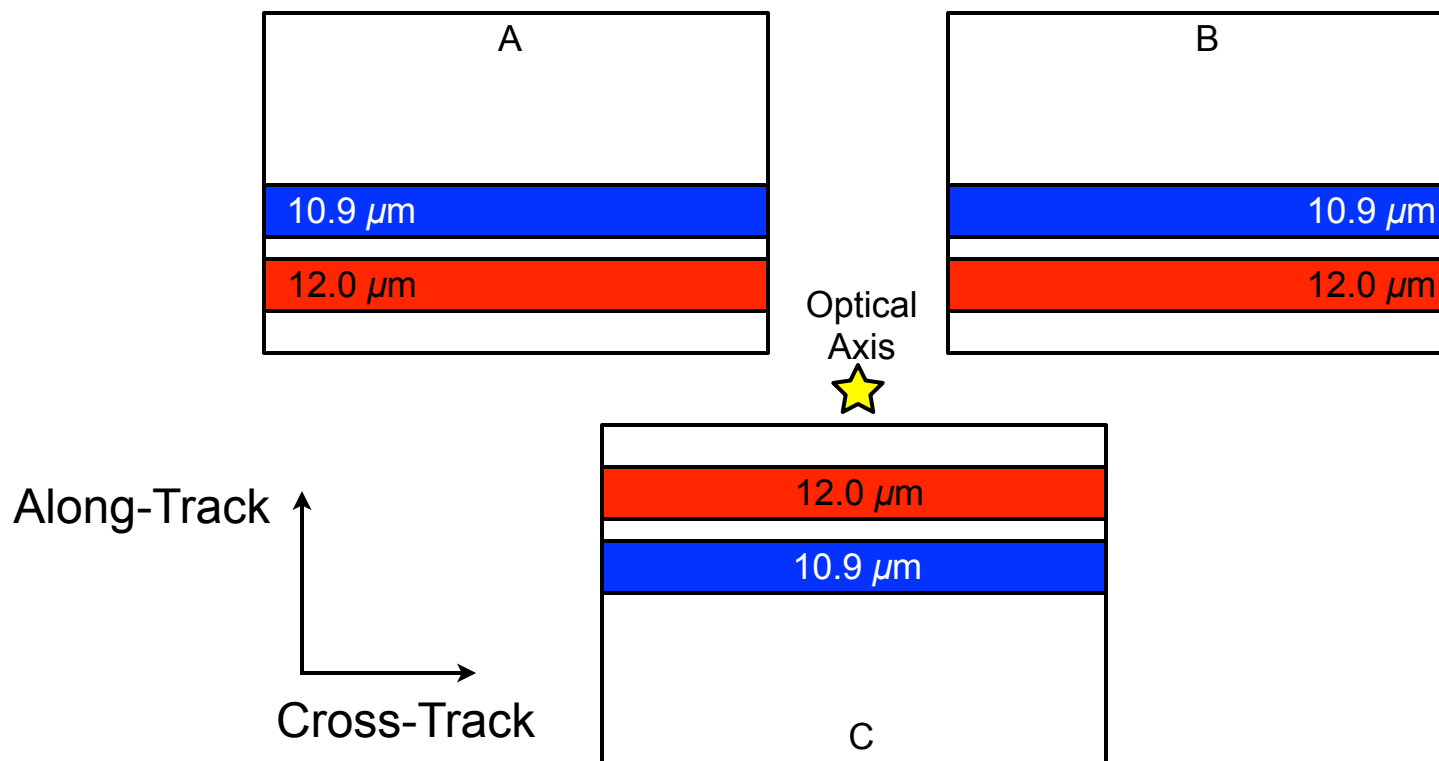
<sup>1</sup>D. Reuter, *et al.*, "The Thermal Infrared Sensor on the Landsat Data Continuity Mission," in *Geoscience and Remote Sensing Symposium (IGARSS)*, 2010 IEEE International, pp. 754-757 (2010).

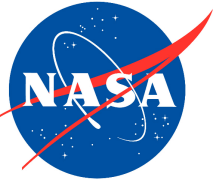
<sup>2</sup>M. Jhabvala, *et al.*, "QWIP-based thermal infrared sensor for the Landsat Data Continuity Mission," *Infrared Physics & Technology* **52**, 424-429 (2009).



# TIRS Focal Plane

- Consists of three QWIP arrays
  - Each QWIP array contains 2 spectral bands, centered on 10.9 and 12.0  $\mu\text{m}$

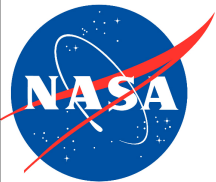




# Purpose of Test

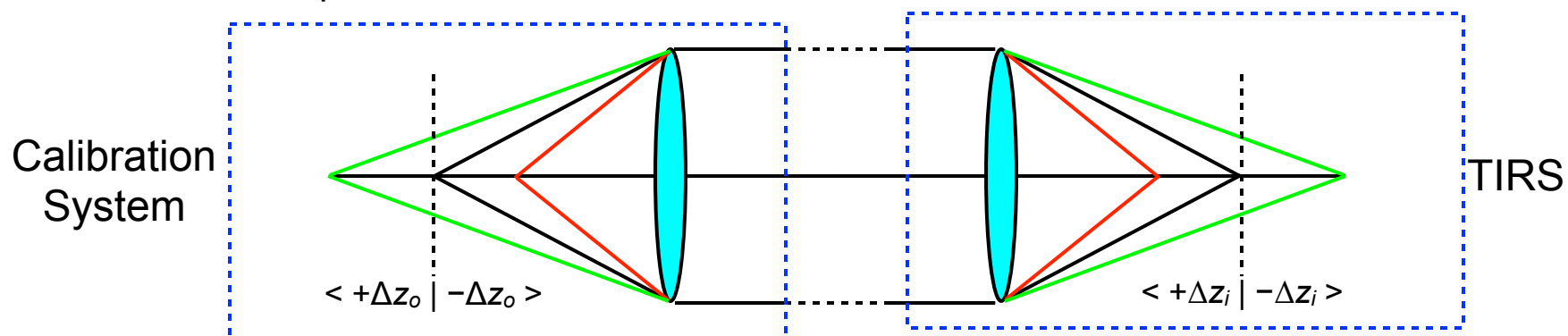
---

- Each QWIP array can be displaced from the nominal focal plane in 3 degrees-of-freedom:
  - Tip about the cross-track axis
  - Tilt about the along-track axis
  - Translation along the optical axis
- No active focus mechanism in the instrument
  - Focal plane must be “Set & Forget” at system integration
  - Some small amount of re-focusing allowed on orbit by controlling telescope temperature
- Need an accurate method of determining system focus for a given focal plane placement
  - Manufacture & install shims to correct

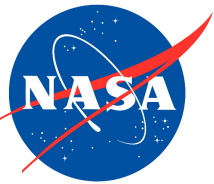


# Methods

- Point-spread function (PSF) focal-sweep data was collected at 18 points across the field-of-view (3 in each band on each QWIP)
  - Defocus achieved by sweeping the *object* point through a limited range along the optical axis



- Each focal sweep was analyzed to determine the nominal defocus of the detector array at that field point
  - Defocus at each field point is converted to tip, tilt and displacement of each QWIP array
- Two methods for determining defocus:
  - Image-based wavefront sensing (phase retrieval)
  - Gaussian-fit model prediction

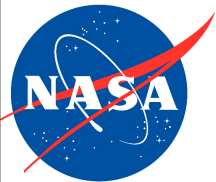


# Methods: Phase Retrieval

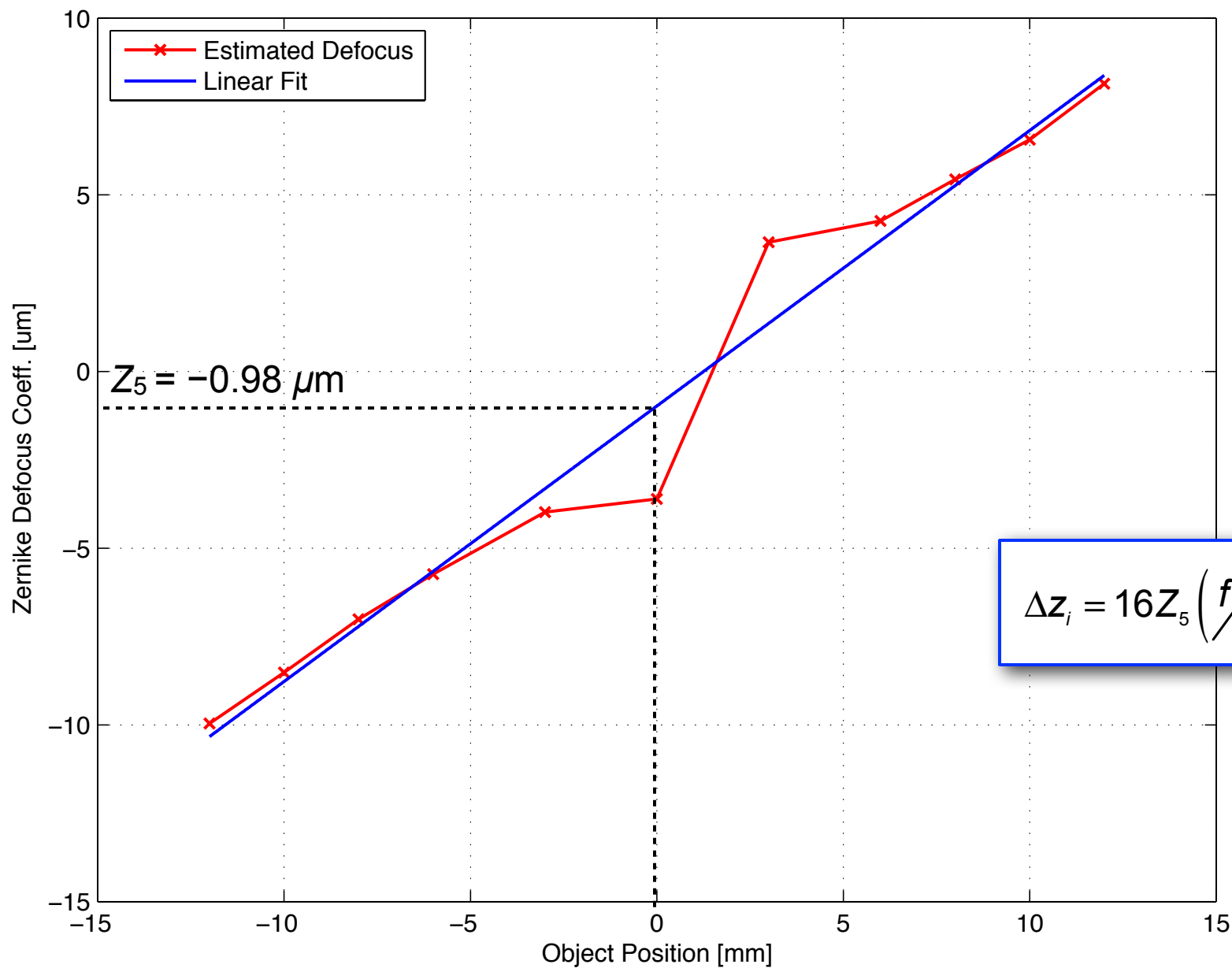
---

- Employs a nonlinear optimization-based algorithm<sup>3</sup>
- Challenging phase-retrieval problem:
  - Undersampled data,  $Q = \lambda(F/\#)/(\text{pixel size}) = 0.78$  at  $\lambda = 12.0 \mu\text{m}$
  - Bandwidth  $(\Delta\lambda / \lambda) \approx 7\%$
  - Limited diversity defocus of  $\approx \pm 0.7\lambda$  at  $12.0 \mu\text{m}$
  - Barely unresolved target: object pinhole diameter = 1 detector pixel
- Jointly optimizes the pupil phase using all the images in the focal sweep, allowing diversity to vary for each image
  - Diversity defocus is implemented as varying amounts of Zernike defocus ( $Z_5$ )

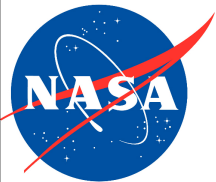
<sup>3</sup>S.T. Thurman and J.R. Fienup, "Complex pupil retrieval with undersampled data," *J. Opt. Soc. Am. A* **26**, 2640-2647 (2009).



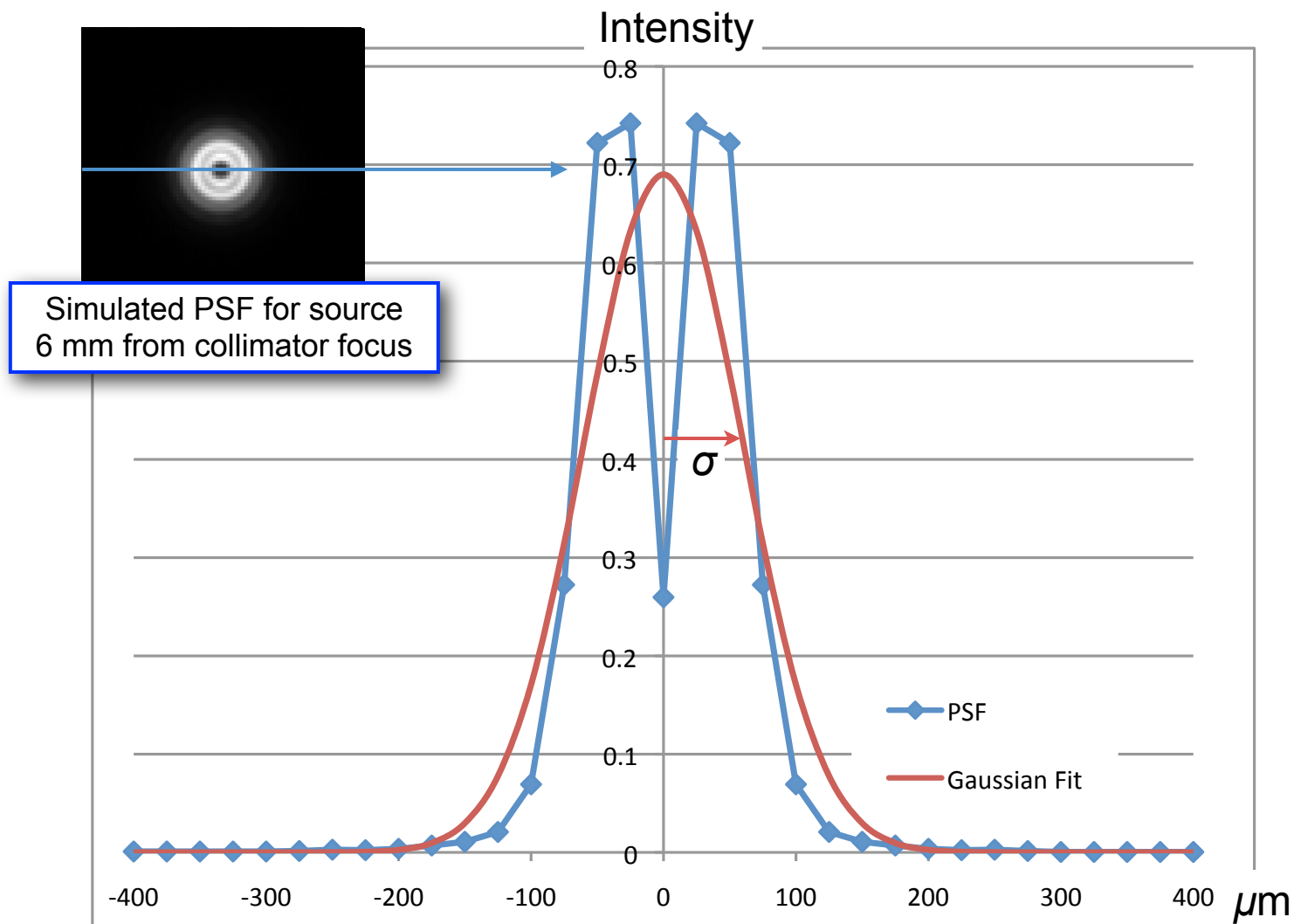
# Methods: Phase Retrieval

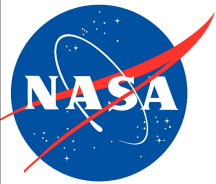






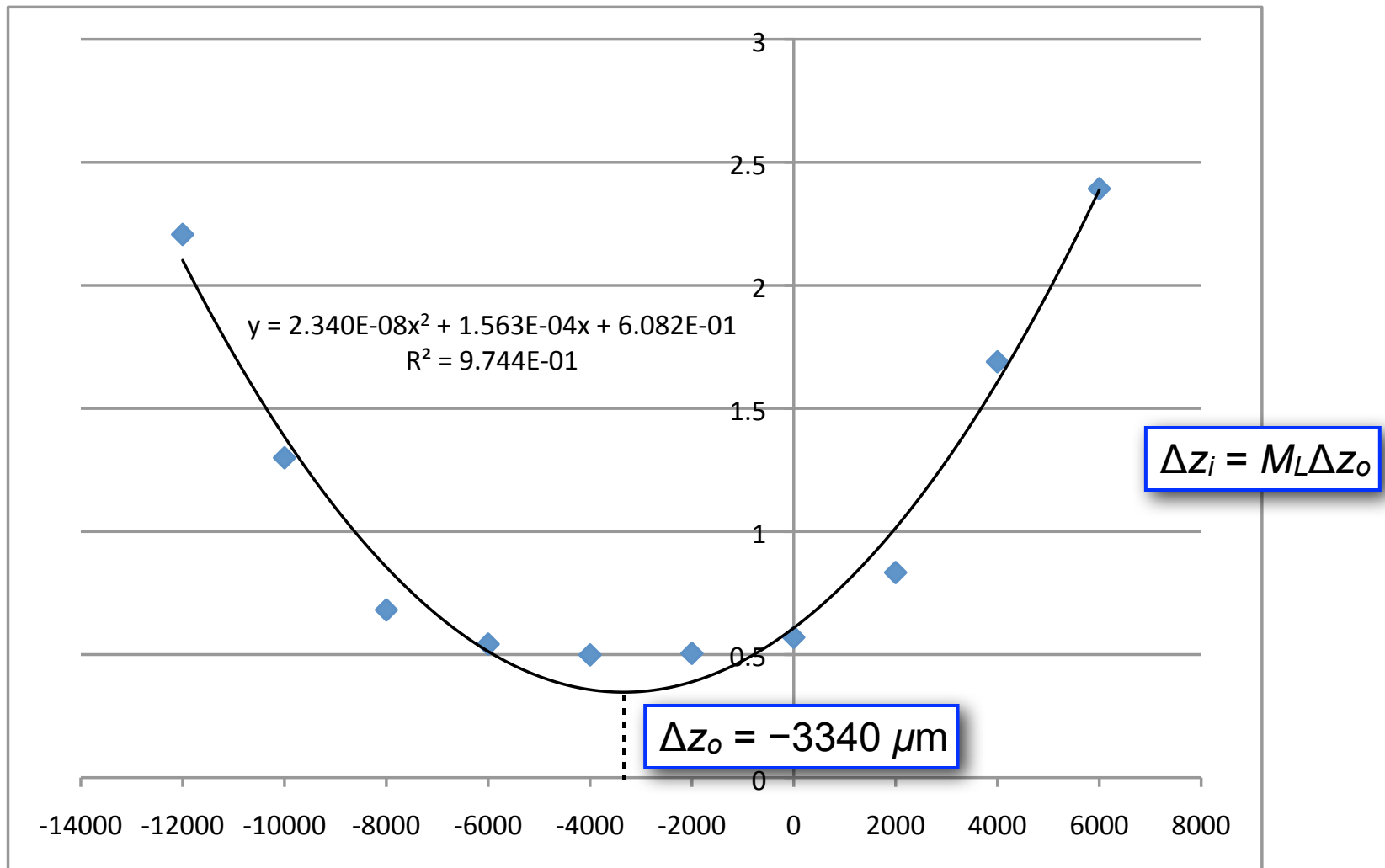
# Methods: Gaussian Fit

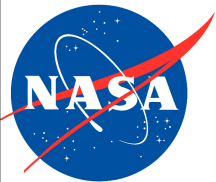




# Methods: Gaussian Fit

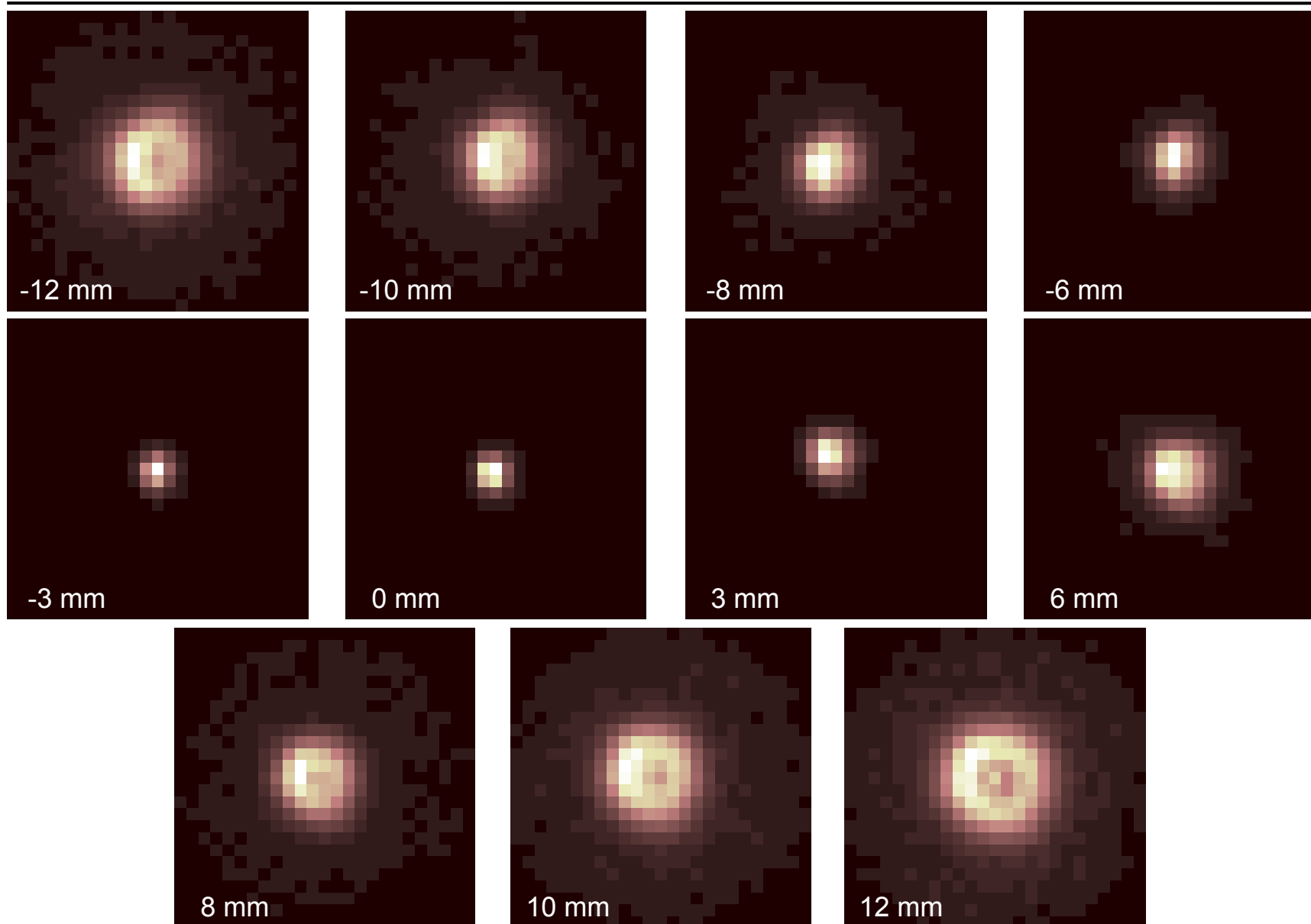
- Plot the Gaussian  $\sigma$  fit for each PSF against source defocus position:

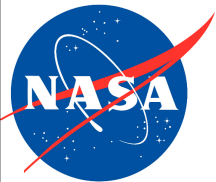




# Data: Single Field Point

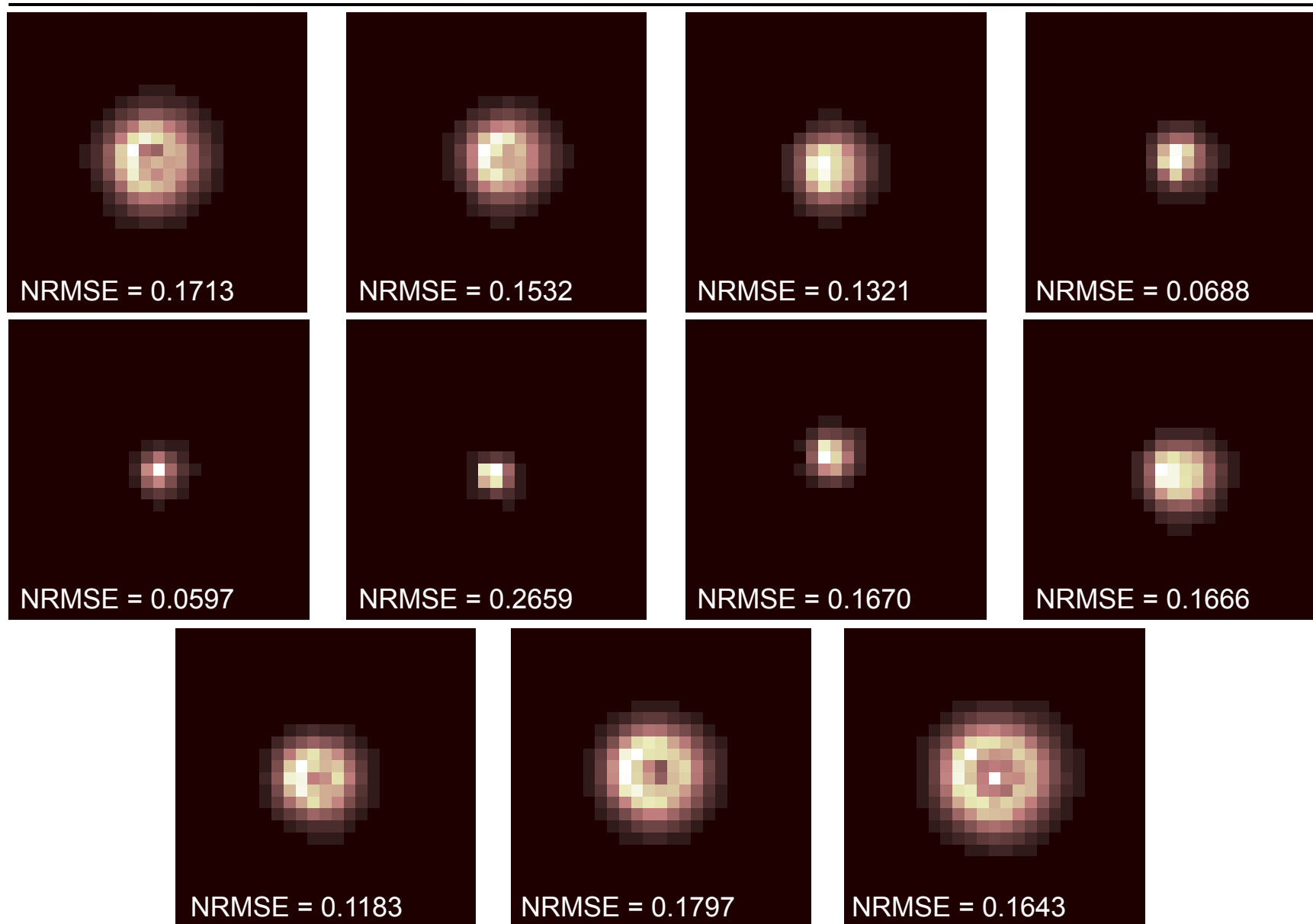
## 12.0 $\mu\text{m}$ Data

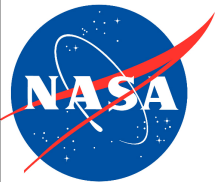




# Results: Estimated PSFs

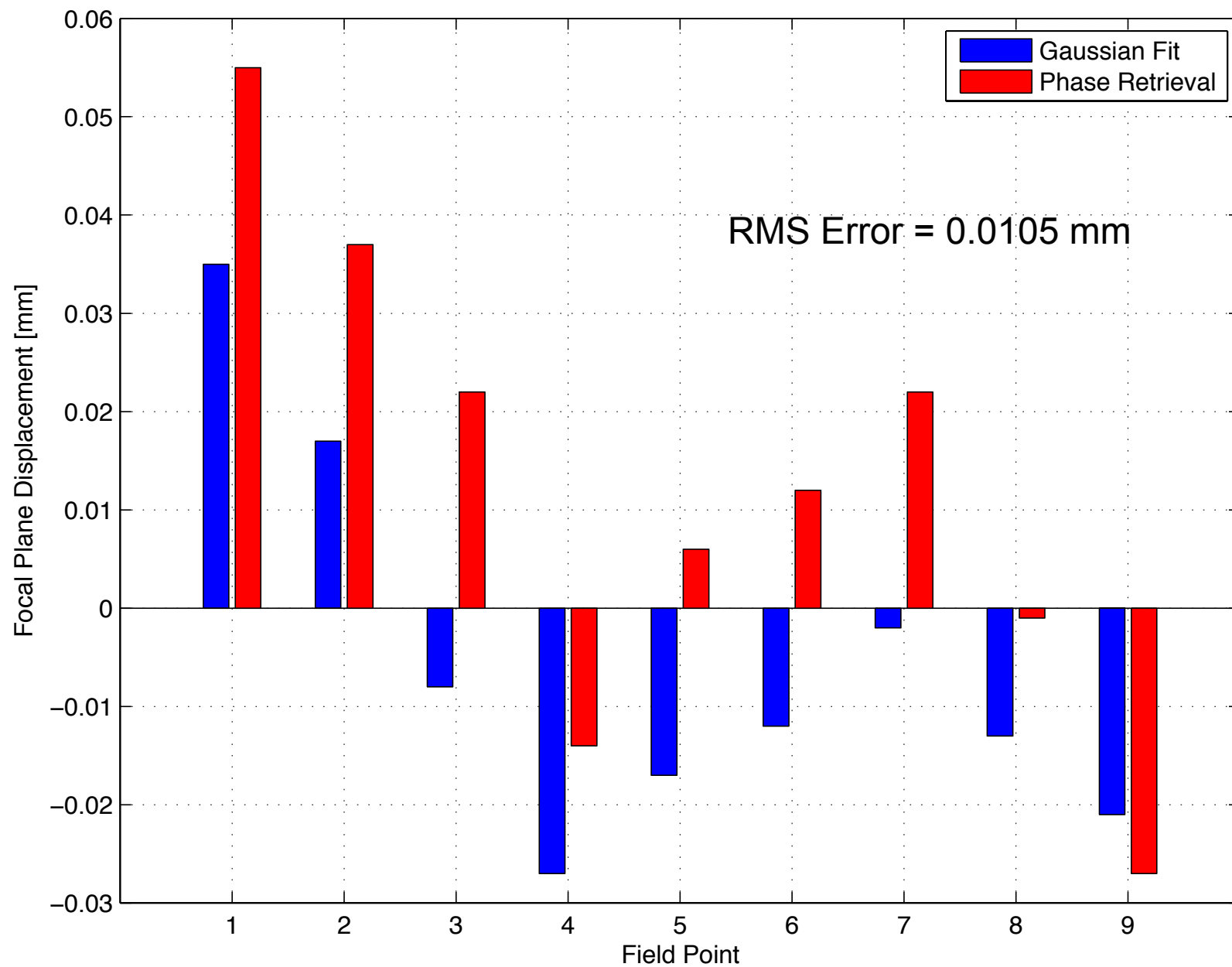
## 12.0 $\mu\text{m}$ Data

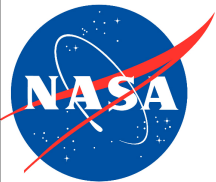




# Results: Comparison

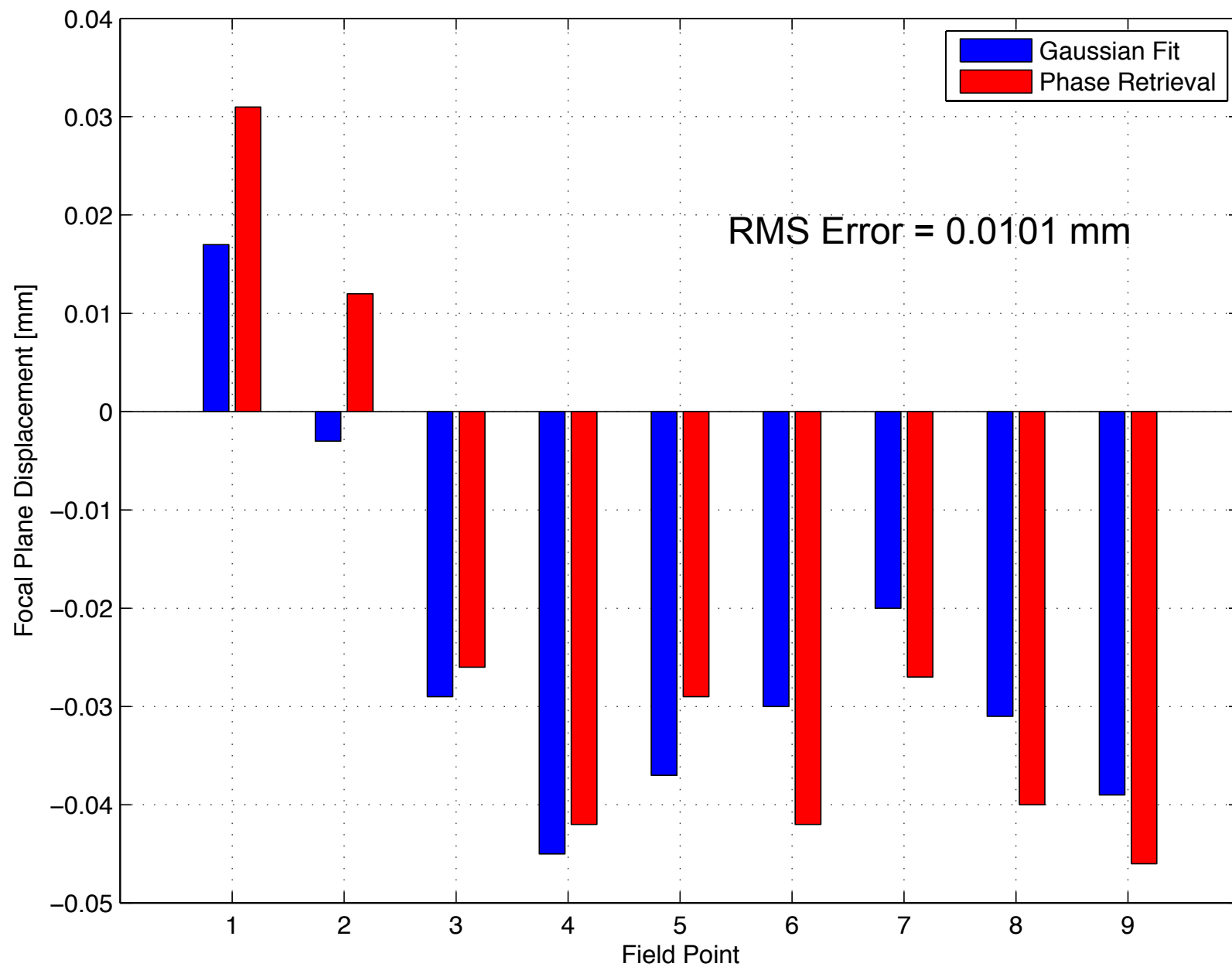
## 10.9 $\mu\text{m}$ Data

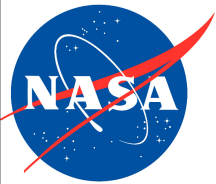




# Results: Comparison

## 12.0 $\mu\text{m}$ Data

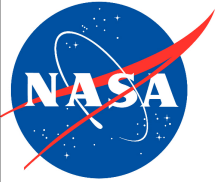




# Conclusion

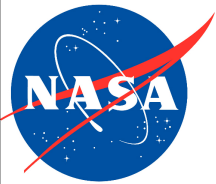
---

- Phase retrieval was used to estimate defocus at various points across the field-of-view
- Challenging wavefront-sensing problem due to undersampled data, minimal diversity, and nearly-resolved object
- Phase-retrieval results were corroborated by an independent Gaussian-fit technique
- Focal-plane displacements from the two techniques agreed to within an RMS error of
  - 0.0105 mm for  $\lambda = 10.9 \mu\text{m}$  data
  - 0.0101 mm for  $\lambda = 12.0 \mu\text{m}$  data



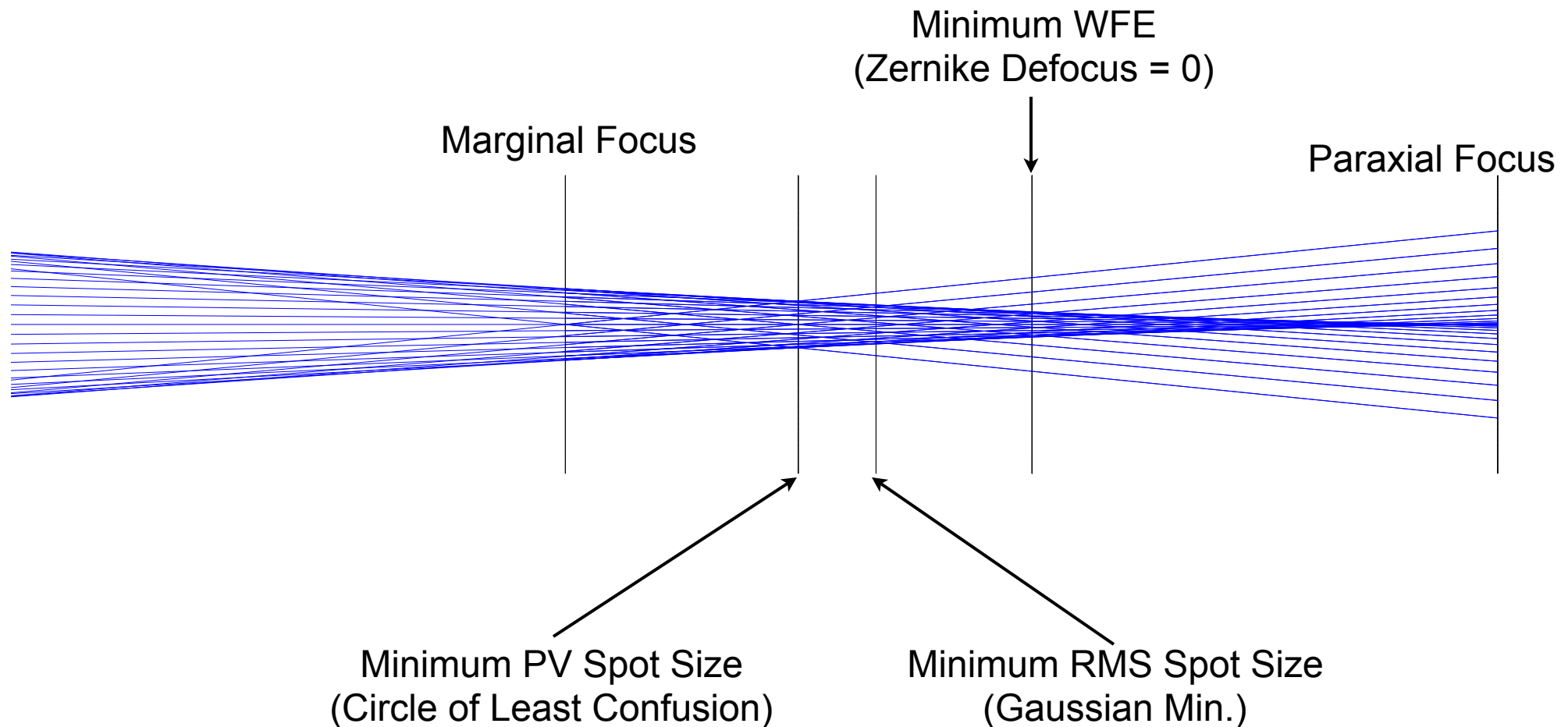
BACKUP





# Definition of “Best Focus” in the Presence of Aberration

---



# Phase Retrieval on Undersampled Data from the Thermal Infrared Sensor (TIRS)

Matthew R. Bolcar and Eric Mentzell

NASA Goddard Space Flight Center, 8800 Greenbelt Rd., Greenbelt, MD 20771  
matthew.bolcar@nasa.gov

**Abstract:** Phase retrieval was applied to under-sampled data from a thermal infrared imaging system to estimate defocus across the field of view (FOV). We compare phase-retrieval estimated values to those obtained using an independent technique.

**OCIS codes:** 100.5070 Phase retrieval, 110.3080 Infrared imaging, 110.6770 Telescopes

## 1. Introduction

Image-based wavefront sensing techniques, such as phase-diverse phase retrieval (PDPR), are becoming increasingly common tools for aligning complicated optical systems, as well as for performing optical metrology at the component level [1, 2]. Generally speaking, image-based techniques are more straightforward to apply when the detected point-spread function (PSF) intensity data is critically sampled ( $Q = 2$ , where  $Q = \lambda(F/\#) / (\text{pixel size})$ ). Recent work has further improved the performance of image-based techniques when applied to undersampled data [3, 4], specifically when  $Q < 1$ .

Building from this earlier work, we have recently performed phase retrieval on under-sampled data collected from NASA's TIRS optical system [5]. We applied the approach of Ref. [3] to estimate the low-order wavefront error of TIRS across the FOV. Of particular interest is the defocus term of the wavefront as it correlates directly to the relative displacement of the detector along the optical axis at each field point.

## 2. System Description

The system under test (SUT) consisted of a 4-element refractive optical telescope and three Quantum Well Infrared Photodetector (QWIP) arrays, operating in a 1- $\mu\text{m}$  bandwidth, centered at 12.0  $\mu\text{m}$  ( $\Delta\lambda/\lambda = 0.08$ ) with a sampling  $Q$  value of 0.78. Blackbody point-source illumination was collimated by an off-axis parabola (OAP) and injected into the SUT. Scanning the point source across the FOV was accomplished by a two-axis steering mirror after the OAP collimator, while introducing defocus was accomplished by moving the point source object along the optical axis about the focal point of the OAP.

In total, 9 field points were examined, the locations of which were determined by active regions on the infrared detector [7]. The range of motion available to the point-source object limited the total amount of defocus that could be introduced to approximately  $\pm 0.7 \lambda$  of Zernike defocus at 12.0  $\mu\text{m}$ . Thus, with the challenges of undersampled PSFs and small defocus diversity, data collected from this imaging system poses a difficult estimation problem.

## 3. Results

A nonlinear optimization phase-retrieval algorithm processed data from all 9 field-points, using 11 diversity defocus images at each field point. The global defocus term was recovered by plotting the Zernike defocus coefficient for each of the diversity images against the corresponding position of the point source relative to the OAP focal point. The zero crossing of a linear fit thus indicates the position at which the point source should be focused onto the detector, and therefore how far the detector is from the focal plane of the optical system.

The detector displacement values obtained using the phase-retrieval algorithm are compared to values obtained from a second, independent method, which was developed to determine shim adjustments for the focal plane assembly. In the alternate method, the detected PSFs were fit to 2-dimensional Gaussian functions, and the  $\sigma$  of the Gaussian fit was plotted against the point-source object's position relative to the OAP focal point. A parabolic fit to this data then determined the source position that gave the minimum  $\sigma$  value. This position for each field point was transferred to an as-built optical model of the SUT and OAP collimator, which allowed for an estimation of the tip, tilt, and defocus of the focal plane assembly. Setting

the source defocus back to 0 in this optical model (i.e. collimated input light) produced an estimate of the defocus at the detector that could be directly compared to the PDPR estimate.

Figure 1 shows a plot of the estimated defocus value for each field point, using both the PDPR technique and the Gaussian fit method. The two techniques are in good agreement across the FOV, with a root-mean-squared difference of 0.010 mm.

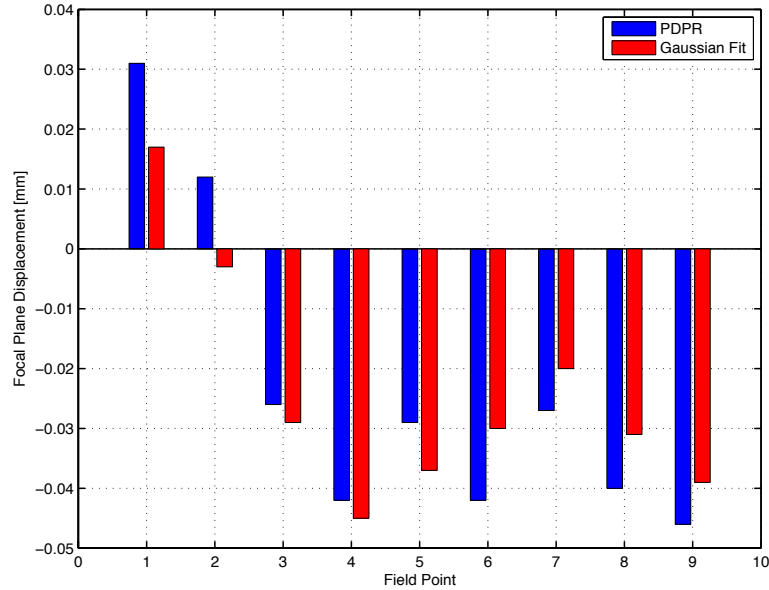


Figure 1 - Comparison of PDPR results with Gaussian fit technique at each of the nine field points.

#### 4. Summary

We present results in which PDPR was used on an undersampled, thermal infrared imaging system with limited diversity defocus to estimate the low-order wavefront error terms across the FOV. The estimated global defocus was used to determine focal-plane displacement and agrees with an independent Gaussian fit technique to within 0.010 mm RMS.

#### 5. References

- [1] G.R. Brady and J.R. Fienup, "Phase retrieval as an optical metrology tool; Technical Digest," in *Optifab: Technical Digest, SPIE Technical Digest*, pp. 139-141 (2005).
- [2] B.H. Dean, D.L. Aronstein, J.S. Smith, R. Shiri, and D.S. Acton, "Phase retrieval algorithm for JWST Flight and Testbed Telescope," *Proc. SPIE* **6265**, 626511 (2006).
- [3] S.T. Thurman and J.R. Fienup, "Complex pupil retrieval with undersampled data," *J. Opt. Soc. Am. A* **26**, 2640-2647 (2009).
- [4] J. S. Smith, D. L. Aronstein, B. H. Dean, and D. S. Acton, "Phase retrieval on broadband and under-sampled images for the JWST testbed telescope," *Proc. SPIE* **7436**, 74360D (2009).
- [5] D. Reuter, C. Richardson, J. Irons, R. Allen, M. Anderson, J. Budinoff, G. Casto, C. Coltharp, P. Finneran, and B. Forsbacka, "The Thermal Infrared Sensor on the Landsat Data Continuity Mission," in *Geoscience and Remote Sensing Symposium (IGARSS), 2010 IEEE International*, pp. 754-757 (2010).
- [6] M. Jhabvala, D. Reuter, K. Choi, C. Jhabvala, and M. Sundaram, "QWIP-based thermal infrared sensor for the Landsat Data Continuity Mission," *Infrared Physics & Technology* **52**, 424-429 (2009).